

A serial study of retinal changes following optic neuritis with sample size estimates for acute neuroprotection trials

Andrew P. D. Henderson,¹ Daniel R. Altmann,² Anand S. Trip,¹ Constantinos Kallis,² Steve J. Jones,³ Patricio G. Schlottmann,⁴ David F. Garway-Heath,⁴ Gordon T. Plant⁵ and David H. Miller¹

1 NMR Research Unit, Institute of Neurology, University College London, London, WC1N 3BG, UK

2 Medical Statistics Unit, London School of Hygiene and Tropical Medicine, Keppel Street, London, WC1E 7HT, UK

3 Department of Clinical Neurophysiology, National Hospital for Neurology and Neurosurgery, London, WC1N 3BG, UK

4 Glaucoma Research Unit, Moorfields Eye Hospital, City Road, London, EC1V 2PD, UK

5 Department of Neurology, The National Hospital for Neurology and Neurosurgery, London, WC1N 3BG, UK

Correspondence to: Andrew P. D. Henderson,
NMR Research Unit, Institute of Neurology,
University College London, London,
WC1N 3BG, UK
E-mail: a.henderson@ion.ucl.ac.uk

Following an episode of optic neuritis, thinning of the retinal nerve fibre layer, which indicates axonal loss, is observed using optical coherence tomography. The longitudinal course of the retinal changes has not been well characterized. We performed a serial optical coherence tomography study in patients presenting with optic neuritis in order to define the temporal evolution of retinal nerve fibre layer changes and to estimate sample sizes for proof-of-concept trials of neuroprotection using retinal nerve fibre layer loss as the outcome measure. Twenty-three patients (7 male, 16 female, mean age 31 years) with acute clinically isolated unilateral optic neuritis were recruited to undergo optical coherence tomography, visual assessments and visual evoked potentials at presentation (median 16 days from onset of visual loss) and after 3, 6, 12 and 18 months. Compared with the clinically unaffected fellow eye, the retinal nerve fibre layer thickness of the affected eye was significantly increased at presentation and significantly reduced at all later time points. The evolution of retinal nerve fibre layer changes in the affected eye fitted well with an exponential model, with thinning appearing a mean of 1.6 months from symptom onset and the rate of ongoing retinal nerve fibre layer loss decreasing thereafter. At presentation, increased retinal nerve fibre layer thickness was associated with impaired visual acuity and prolonged visual evoked potential latency. Visual function after 12 months was not related to the extent of acute retinal nerve fibre layer swelling but was significantly associated with the extent of concurrent retinal nerve fibre layer loss. Sample size calculations for placebo-controlled trials of acute neuroprotection indicated that the numbers needed after 6 months of follow up are smaller than those after 3 months and similar to those after 12 months of follow-up. Study power was greater when investigating differences between clinically unaffected and affected eyes rather than retinal nerve fibre layer thickness of the affected eye alone. Inflammation in the optic nerve and impaired axonal transport (implied by retinal nerve fibre layer swelling) are associated with visual dysfunction and demyelination (long visual evoked potential latency) during acute optic neuritis. Retinal nerve fibre layer thinning is usually evident within 3 months. Optical coherence tomography-measured retinal nerve fibre layer loss after 6 months is a suitable outcome measure for proof-of-concept trials of acute neuroprotection in optic neuritis.

Keywords: optic neuritis; optical coherence tomography; sample size estimates; retinal nerve fibre layer; axonal loss

Abbreviations: logMAR = logarithm of the minimum angle of resolution; RNFL = retinal nerve fibre layer; TES = total error score

Introduction

The initial presentation and early clinical course of multiple sclerosis, in most patients, is characterized by acute episodes of neurological dysfunction that are known as relapses. Such episodes are due to development of new inflammatory demyelinating lesions in central nervous system white matter. While most relapses will be followed by a partial or complete recovery of neurological function, a minority will result in permanent functional deficits. It is thought that axonal damage and loss occurring in the acute inflammatory lesion are the main pathological substrates of incomplete recovery (Ferguson *et al.*, 1997; Trapp *et al.*, 1998).

One of the most common and characteristic syndromes at the onset or during the course of the relapsing remitting phase of multiple sclerosis is an episode of acute optic neuritis, which results from the development of an inflammatory demyelinating lesion in the optic nerve. The anterior visual pathway, including the optic nerve and retinal nerve fibre layer (RNFL), has been suggested as a particularly suitable site for studying the pathophysiology and treatment of acute inflammatory demyelinating central nervous system lesions that occur in optic neuritis and multiple sclerosis (Kolappan *et al.*, 2009). The functions of the optic nerve are quantifiable both clinically (with quantitative tests of visual function including acuity, fields and colour vision) and electrophysiologically (by measuring the visual evoked potential). The optic nerve can also be imaged using MRI to elucidate the extent and nature of structural abnormalities in the symptomatic lesion. Importantly, the development of axonal loss can also be inferred by imaging the RNFL using optical coherence tomography.

In a serial study of the optic nerve following a single episode of optic neuritis, Hickman and colleagues (2004a) found initial swelling of the diseased optic nerve, which declined over time with the nerve being atrophic compared with the fellow eye after 1 year. Using the measurements of the optic nerve atrophy to infer axonal loss is unfortunately confounded by accompanying myelin loss. However, the axons of the retinal ganglion cells, which form the optic nerve, are unmyelinated in the RNFL. In the RNFL, the axons form the bulk of the tissue (Ogden, 1984) and so reductions in its thickness are likely to relate more directly to loss of ganglion cell axons (the same fibres that travel in the optic nerve). Whilst it is known that retinal vessels attenuate with retinal atrophy, blood vessels form only a small proportion of retinal tissue (Hood *et al.*, 2008). The RNFL can be quantified in life with optical coherence tomography (Huang *et al.*, 1991).

Axonal loss in the retina, as a consequence of optic neuritis, can sometimes be directly seen in the retina (Frisén and Hoyt, 1974; Sharpe and Sanders, 1975), and has been documented and quantified using optical coherence tomography in cross-sectional studies of patients with multiple sclerosis (Parisi *et al.*, 1999) and clinically isolated optic neuritis (Trip *et al.*, 2005; Costello *et al.*,

2006; Klistorner *et al.*, 2008). Costello and colleagues (2008) studied a group of patients at varying intervals following a single episode of optic neuritis, and observed no further RNFL loss 6 months after symptoms began.

There have been no systematic longitudinal studies of acute optic neuritis using optical coherence tomography to follow changes over time in the RNFL, and no studies have serially looked at changes in the macula. Whilst the study by Costello and colleagues (2008) was predominantly cross-sectional at various time points, it included a subset of 20 patients followed from one to 3 months after onset of symptoms up to 12 months. It was unclear, however, what the exact nature of the time course was, and whether swelling of the RNFL (as seen in two other small cohorts) (Menke *et al.*, 2005; Pro *et al.*, 2006) was a characteristic early finding. Hickman and colleagues (2004a) observed ongoing loss of optic nerve mean area more than a year after unilateral optic neuritis and it is unclear whether this is also seen in the RNFL and macula.

We designed a prospective, systematic longitudinal optical coherence tomography study in a cohort of patients presenting with optic neuritis, the aims of which were to:

- (a) characterize, with appropriate statistical models, the time-course of (i) early RNFL swelling that reflects inflammation in the optic nerve and/or interruption of axonal transport (Kallenbach *et al.*, 2010); and (ii) subsequent RNFL thinning that implies axonal loss following optic neuritis;
- (b) investigate whether RNFL swelling during acute optic neuritis predicts later axonal loss and visual outcome;
- (c) report serial macular volume changes following acute optic neuritis; and
- (d) estimate sample sizes for clinical trials of neuroprotective agents in acute optic neuritis that use optical coherence tomography-measured RNFL loss as the outcome measure.

Materials and methods

Patients

Twenty-three patients with their first episode of acute unilateral optic neuritis (7 male, 16 female, median age 31 years, range 21–49 years) were recruited from the neuro-ophthalmology clinic, Moorfields Eye Hospital, London. There was no prior history of clinical events suggesting demyelination elsewhere in the central nervous system, i.e. patients had clinically isolated unilateral optic neuritis at study entry. The delay from onset of symptoms to first study examination was 16 days, range 10–32 days. All patients were examined acutely, and then at 3, 6, 12 and 18 months after onset of symptoms. At each visit, a neurological assessment was undertaken and brain MRI was obtained and analysed for the presence of lesions compatible with

demyelination and for fulfilment of the McDonald criteria for multiple sclerosis (Polman *et al.*, 2005). Some patients had missing time points. No patient had recurrent or contralateral optic neuritis during or prior to the study period.

Approval was obtained for the study from the National Hospital for Neurology and Neurosurgery and University College London Institute of Neurology Joint Research Ethics Committee; informed consent was obtained from each patient, in accordance with the Declaration of Helsinki.

Optical coherence tomography

Optical coherence tomography images were acquired with a time domain optical coherence tomography (Stratus OCT Model 3000; Carl Zeiss Meditec, Dublin, CA, USA). RNFL images were acquired by taking three circular 3.4 mm scans, centred on the optic disc, the mean of which was used to express RNFL thickness (Fast RNFL thickness protocol). The thicknesses of the quadrants of the RNFL were automatically calculated by the optical coherence tomography device software. Variability of the size of the optic disc accounts for a small proportion of the variability of the RNFL thickness (Baleanu *et al.*, 2009) and adjusting the scan circle diameter does not account for this variation (Kaushik *et al.*, 2009); accordingly, we did not adjust the RNFL measures for disc diameter. Macular thickness maps were acquired by making six radial scans centred on the fovea, and by construction of a map from these scans (Fast macular thickness map scanning protocol). Optical coherence tomography images are given a signal strength by the Stratus optical coherence tomography device, with a maximum of 10. Optical coherence tomography images were rejected if an individual eye was <7, the inter-eye signal strength difference was >2, or if the difference in signal strength between baseline and follow-up scans was >2.

Twelve control subjects (five male, seven female, median age 31 years, range 24–50 years) were also imaged, on two occasions, a median of 552 days (range 350–907 days) apart, with the scanning dates spanning a similar duration of time as the study of optic neuritis patients.

Visual assessments

Patients were examined at each visit. Visual acuity was measured (unaided, with appropriate refraction or with pinhole correction) using a retro-illuminated early treatment diabetic retinopathy study chart and recorded as the 4 m logarithm of the minimum angle of resolution (logMAR) acuity (Ferris *et al.*, 1982). In addition, Sloan 1.25% contrast early treatment diabetic retinopathy study charts were used at 4 m to calculate the equivalent low-contrast visual acuity. When no letters could be identified correctly, a score of 1.7 was assigned (Optic Neuritis Study Group, 1991). Colour vision was measured with Farnsworth-Munsell 100 Hue colour test (Farnsworth, 1943) and analysis was performed on the square root of the total error score ($\sqrt{\text{TES}}$), as this is normally distributed. Central visual field sensitivity was analysed using the 30-2 program on the Humphrey field analyser (Carl Zeiss Meditec, Dublin, CA, USA). Wide angle lenses were used to correct refractive errors when necessary. The overall field mean deviation was derived from control data provided by the manufacturer. A mean deviation of -35 dB was assigned when vision was too poor to attempt the test (Kupersmith *et al.*, 2002). For the purposes of comparing the models of RNFL thickness and macular volume changes, two subgroups were defined according to the degree of visual recovery at or after 12 months. 'Good' visual recovery was defined as a logMAR acuity ≤ 0.1 and 'poor' recovery as logMAR > 0.1 . The good

level of recovery is exhibited by a majority of optic neuritis patients (Beck *et al.*, 1994), and is a level at which at least one of colour vision, visual field sensitivity and contrast sensitivity are likely to be normal (Trobe *et al.*, 1996).

Visual evoked potentials

Patient central field pattern reversal visual evoked potentials were measured on each study visit using methods previously described (Brusa *et al.*, 2001).

Statistical methods

Paired *t*-tests were used to assess differences between affected and fellow eyes in patients at fixed time points. Comparisons of patients' affected and fellow eyes with control eye values were made by unpaired *t*-tests between each patient eye and a single randomly selected eye per control.

Changes in controls' retinal optical coherence tomography measures over time were assessed using mixed effects linear regression. For comparison with patients' clinically unaffected eyes, patient indicator time interaction terms were used.

Linear regression was used to investigate relationships between retinal measures and quantitative measures of vision and visual evoked potentials. Where residuals could not be assumed to be normal, non-parametric bias-corrected bootstrap (Efron and Tibshirani, 1993) estimates (1000 replicates) were obtained. The bootstrap randomly resamples from the data to produce confidence limits from the observed variability, rather than use parametrically derived standard errors; it is standardly used when either parametric assumptions do not hold, or when estimating functions of several parameters where there is no theoretically derivable standard error.

The time course for changes in retinal values was assessed using an exponential model (Snedecor and Cochran, 1989) similar to that used previously for visual recovery (Hickman *et al.*, 2004b) and serial optic nerve MRI changes (Hickman *et al.*, 2004a); such exponential models are optimal for modelling an early rapid change which slows to settle at an eventual final value. Such a time course is plausible *a priori* for visual function, but less so for RNFL and macular volume; however, the raw data supported this type of course (Figs 1 and 3). As a precaution, two alternative models were examined (polynomial time models were not considered as they tend artefactually to impose curves at the extremes): (i) regressing retinal values on log time,

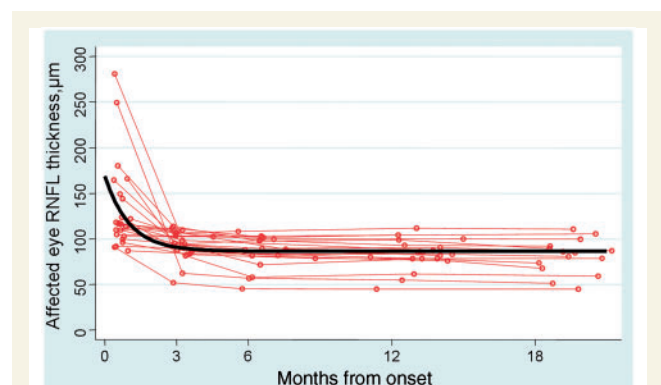


Figure 1 Affected eye RNFL thickness with fitted exponential model, all patients.

which has a similar decelerating rate as an exponential model but with continued decline (i.e. without settling at a final value); and (ii) a saturated means model which, by simultaneously fitting the mean retinal value at each time point, is the best possible fit. Although this latter model has the disadvantage of not being useful for interpretation, since it treats retinal values as unrelated over time, it is a convenient benchmark against which to assess the fit of other models. R^2 -values were used to compare model fit. Exponential modelling of both the RNFL and macular volume was carried out both for the affected eye retinal value and for the difference between the affected eye and the baseline fellow eye value.

The algebraic form of the exponential model used (shown here without the detailed error structure that is described in the online supplementary material) is:

$$y = \alpha + \beta \exp(-\gamma t), \quad (1)$$

where y , the response variable, is the nerve fibre layer thickness, t is months from onset, α represents the asymptote, or predicted eventual RNFL thickness, β is the absolute value of the drop between the initial value and the asymptote, and γ controls the tightness of the curve. The model yields: (i) an estimate of the final value (not necessarily the level at the last assessment), given by α ; (ii) the rates of change at a given time, given by $-\beta\gamma \exp(-\gamma t)$; (iii) times to achieve a given fraction d of the total change from start to final value, given by $-(1/\gamma) \ln(1-d)$; and (iv) times to achieve zero value, given by $(1/\gamma) \ln(-\beta/\alpha)$; this was calculated when y was affected minus baseline fellow eye value, where zero estimates a point where atrophy begins relative to the fellow eye value. Results are reported from a hierarchical model of this form, implemented in Windows Bayesian interference Using Gibbs Sampling (WinBUGS) software (Lunn *et al.*, 2000) with details given in the Supplementary material. The modelling assumes that any missing data points are missing at random.

Sample size estimates for two-arm trials measuring RNFL of 3, 6 and 12 month duration were based on means and standard deviations obtained directly from the data at the three time points for affected eye RNFL and affected minus baseline fellow RNFL; and on Pearson correlation coefficients between baseline fellow and affected RNFL values at the three time points. Estimates were calculated for two-tailed tests at $\alpha=0.05$, for 80 and 90% power, to detect treatment effects of from 20 to 80%, where 100% treatment effect was taken as the mean difference: follow-up (3, 6 or 12 month) affected eye RNFL minus baseline fellow eye RNFL. Confidence intervals (CIs) for selected sample sizes were obtained using the bootstrap method described above. Calculations, using standard methods (Senn, 1997) were for three between-arm comparisons, in order of increasing theoretical efficiency.

- (i) Method A: mean follow-up affected RNFL, using follow-up affected RNFL standard deviation (and ignoring fellow eye value, as would be advisable when there is a history of prior optic neuritis in the fellow eye).
- (ii) Method B: mean difference follow-up affected RNFL minus baseline fellow eye RNFL, using the standard deviation of this difference.
- (iii) Method C: mean follow-up affected RNFL adjusted for baseline fellow eye RNFL, using the follow-up affected RNFL standard deviation and the follow-up affected versus baseline fellow Pearson correlation coefficient (Senn, 1997). Sample sizes for Method C are functions of the treatment effect, the affected RNFL standard deviation and the baseline fellow versus follow-up affected eye RNFL correlation coefficient.

All statistical analyses except the hierarchical exponential model were performed in Stata 9.2 (Stata Corp, College Station, TX).

Results

Patient clinical details

During the study, four patients experienced a second clinical episode of demyelination (all in their spinal cord) and were diagnosed with multiple sclerosis. A further eight patients did not experience a second clinical episode of demyelination but fulfilled the McDonald criteria for the diagnosis of multiple sclerosis (Polman *et al.*, 2005) on the basis of changes on brain MRI. Of the remainder of the patients, nine had MRI changes consistent with inflammatory demyelination, but not fulfilling the McDonald criteria. Two patients had no brain lesions. No patient received intravenous glucocorticosteroids during the acute optic neuritis episode and none were treated with multiple sclerosis disease modifying therapy during the course of the study.

Patient clinical measures in affected nerves

At baseline, in affected eyes, the mean [standard deviation (SD)] logMAR acuity was 0.52 (0.73) (median 0.04, range -0.10 to 1.70), the mean (SD) sloan 1.25% contrast acuity was 1.30 (0.46) (median 1.66, range 0.52 to 1.70), the mean (SD) whole field mean deviation was -13.0 (12.8) (median -7.0 , range -33.0 to 0.0) and the mean (SD) $\sqrt{\text{TES}}$ was 19.3 (11.1) (median 13.3, range 7.8–36.6). Twenty-one of the 23 patients had eye pain at presentation, 20 had a relative afferent pupillary defect, and eight had swelling of the optic disc visible with a hand held ophthalmoscope.

At 12 months, in affected eyes, the mean (SD) logMAR acuity was 0.08 (0.25) (median 0.02, range -0.12 to 0.94), the mean (SD) sloan 1.25% contrast acuity was 0.97 (0.48) (median 0.78, range 0.44 to 1.7), the mean (SD) whole field mean deviation was -5.0 (6.1) (median -4.3 , range -27.0 to 0.25) and the mean (SD) $\sqrt{\text{TES}}$ was 12.3 (5.0) (median 11.3, range 6.6 to 22.7). Thirteen of the patients had developed pallor of the optic disc in the affected eye and six had a residual relative afferent pupillary defect. Five of the patients were classified as having a poor visual recovery (logMAR acuity > 0.1).

Control retinal measures

At baseline, the median RNFL thickness for controls was $106.7 \mu\text{m}$ (mean 105.4 , SD 9.7 , range 90.1 to 118.1). At 18 months, the mean RNFL thickness was $104.1 \mu\text{m}$ (SD 11.3). This decrease was not significant [mean loss $0.004 \mu\text{m}$ per day, 95% CI 0.009 , 0.000 ; $P=0.076$].

At baseline, the mean macular volume was 6.83 mm^3 (SD 0.28). At 18 months, the mean macular volume was 6.88 mm^3 (SD 0.28), and the increase was not significant (mean increase 0.0001 mm^3 per day, 95% CI 0.0000 , 0.0002 ; $P=0.104$).

Patients' healthy contralateral (fellow eye) retinal measures

At baseline, the median RNFL thickness for the patients' healthy unaffected eyes was 101.0 μm (mean 103.0 μm , SD 9.6, range 88.3–124.2), not significantly different from healthy control values ($P=0.711$) (Table 1). There was a small, but significant decrease over time in fellow eye RNFL (mean loss 0.005 μm per day, 95% CI 0.002, 0.008; $P=0.002$), but this gradient was not significantly different from that seen in controls (patient-control gradient difference $-0.0004 \mu\text{m}$ per day, 95% CI -0.0055 , 0.0046; $P=0.861$).

The mean macular volume of patients' fellow eyes was 6.89 mm^3 (SD 0.39), not significantly different from healthy control values ($P=0.670$). There was no significant change over time in patient fellow eye macular volume values (gradient of change -0.0001mm^3 per day, 95% CI -0.0002 , 0.000; $P=0.055$), and there was no difference in patient fellow eye and healthy control gradients (patient-control gradient difference -0.0001 , 95% CI -0.0003 , 0.0000; $P=0.217$).

Patients' affected optic nerve retinal measures

RNFL thickness

At baseline, the median thickness of patients' diseased RNFL was 116.5 μm (mean 132.8 SD 48.8, range 86.9–280.9), which was significantly increased compared to fellow eyes ($P=0.006$), and on the borderline of significance when compared with control eyes ($P=0.050$). The estimated values of the exponential model parameters were: α 86.52 (95% CI: 79.11, 94.4; $P<0.05$), β 82.22 (CI: 43.23, 122.4; $P<0.05$), γ 0.9764 (CI: 0.8307, 1.182; $P<0.05$) (Fig. 1).

The estimated rates of change in RNFL thickness in patients' affected eyes are shown in Table 2. Using this model the mean time to 50% loss from initial values to the asymptote value was 0.72 months (95% CI 0.59, 0.83; $P<0.05$), the mean time to 90% loss was 2.38 months (95% CI 1.95, 2.77; $P<0.05$) and 99% of the loss from the initial value to the asymptotic value had occurred by a mean of 4.75 months (95% CI 3.90, 5.54; $P<0.05$). At final follow-up, affected eye RNFL thickness was significantly smaller than controls ($P<0.001$).

The time of first detectable atrophy compared with the baseline fellow eye value was 1.64 months (95% CI 0.96, 2.32; $P<0.05$). The parameter estimates for this portion of the model (affected minus baseline RNFL thickness) were: α -16.55 , β 83.14 and γ 0.983 (Fig. 2).

When the patients were divided by visual recovery status, there was no significant difference between baseline RNFL thickness ($P=0.980$), but those with a poor recovery ($n=5$) had a larger drop from baseline to 3 month RNFL ($P=0.002$). Those patients with poor recovery had a significantly lower asymptote than those with a good recovery (α_{NR} 66.78 95% CI 54.32, 79.43; α_{R} 92.5 95% CI 85.69, 99.36; difference in α 25.72, 95% CI 11.06, 39.36; $P<0.05$). The β and γ parameters could not be reliably estimated in the subgroups.

Table 1 Patient RNFL measures at study time points

	Baseline <i>n</i> = 22	3 months <i>n</i> = 19	6 months <i>n</i> = 17	12 months <i>n</i> = 19	18 months <i>n</i> = 17
Median days elapsed since symptom onset (range)	16 (10, 32)	92 (76, 136)	195 (167, 264)	393 (333, 450)	582 (368, 636)
Affected eye RNFL thickness, μm					
Median, (range)	116.4 (86.9, 280.9)	94.6 (52.2, 113.7)	88.5 (45.2, 108.2)	85.1 (45.1, 111.8)	84.7 (44.8, 110.7)
Mean (SD)	132.0 (49.8)	92.8 (16.2)	85.3 (18.3)	83.3 (16.3)	82.0 (18.6)
Fellow eye RNFL thickness, μm					
Median, (range)	101.1 (88.3, 124.2)	102.5 (85.9, 122.6)	102.8 (89.0, 123.1)	98.3 (84.6, 123.3)	101.6 (83.0, 123.0)
Mean (SD)	103.0 (9.6)	103.3 (10.4)	103.7 (11.4)	101.6 (11.6)	101.2 (11.9)
Affected eye macular volume, mm^3					
Median, (range)	6.90 (6.16, 8.11)	6.52 (5.63, 7.26)	6.34 (5.46, 7.31)	6.31 (5.56, 7.27)	6.40 (5.55, 7.33)
Mean (SD)	6.96 (0.43)	6.58 (0.38)	6.38 (0.40)	6.34 (0.40)	6.35 (0.46)
Fellow eye macular volume, mm^3					
Median, (range)	6.78 (6.30, 7.87)	6.89 (6.26, 7.88)	6.83 (6.34, 7.49)	6.83 (6.34, 7.45)	6.83 (6.43, 7.59)
Mean (SD)	6.89 (0.39)	6.88 (0.36)	6.83 (0.29)	6.85 (0.31)	6.80 (0.29)

Table 2 Estimated rates of reduction in RNFL thickness

Time (from first measurement)	Rate of atrophy ($\mu\text{m}/\text{month}$)	95% CI	P-value
At first measurement	−80.6	−131.3–40.9	<0.05
15 days	−49.2	−76.2–25.5	<0.05
1 month	−30.1	−44.8–15.8	<0.05
3 months	−4.3	−6.6–2.2	<0.05
4 months	−1.6	−2.7–0.7	<0.05
5 months	−0.6	−1.1–0.2	<0.05
6 months	−0.2	−0.5–0.1	<0.05
12 months	−0.0009	−0.003–0.00007	<0.05

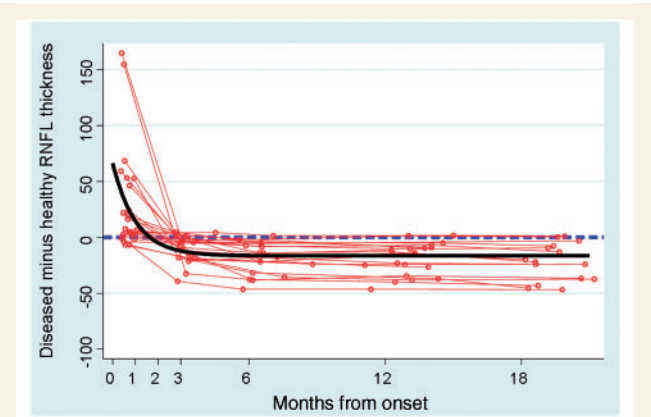


Figure 2 Affected minus baseline fellow RNFL thickness with fitted exponential model. The interrupted line represents the level at which the affected and fellow eye have the same value.

Macular volume

At baseline, patients' affected eye macular volume (median macular volume 6.90 mm^3 , range $6.16\text{--}8.11$; mean macular volume 6.91 mm^3 , SD 0.36) was similar to the fellow eye macular volume (median fellow eye macular volume 6.78 , range $6.54\text{--}7.36$; mean macular volume 6.89 , SD 0.39 , $P=0.371$), and to the control eye value ($P=0.697$). The change in macular volume over time was modelled by an exponential function with the parameters as defined for RNFL. The absolute values of the parameters were: α 6.35 (95% CI: 6.14 , 6.55 ; $P<0.001$), β 0.789 (95% CI: 0.522 , 1.085 ; $P<0.001$), γ 0.418 (95% CI: 0.294 , 0.686 ; $P<0.001$) (Figs 3, 4).

The estimated rates of change in patients' affected eye macular volume are shown in Table 3. The predicted time to 50% loss of macular volume was 1.66 months (95% CI 0.99 , 2.29 ; $P<0.05$), and to 90 and 99% loss of macular volume 5.52 months (95% CI 3.28 , 7.61 ; $P<0.05$) and 11.03 months (95% CI 6.56 , 15.22 ; $P<0.05$), respectively. At final follow-up, affected eye macular volume was significantly smaller than controls ($P<0.001$).

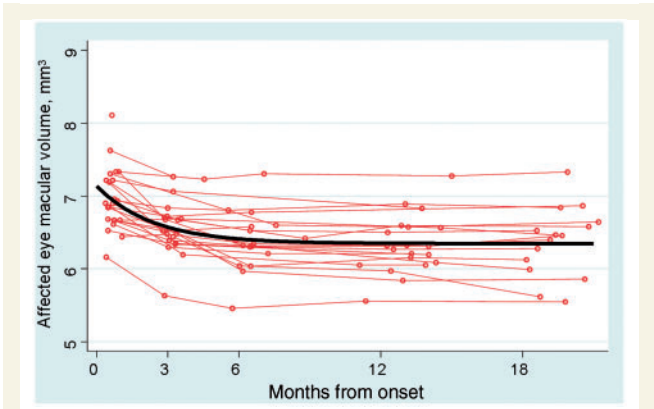


Figure 3 Affected eye macular volume with fitted exponential model, all patients.

Model fit

The exponential model was found to fit the data well: for both RNFL and macular volume, R^2 goodness-of-fit values for the exponential model (RNFL 0.351 , macular volume 0.272) were only slightly lower than for the saturated means model (RNFL 0.352 , macular volume 0.273) but substantially higher than for the log time model (RNFL 0.320 , macular volume 0.260), thus justifying the choice of exponential model.

Relationship of early loss to final retinal outcome

Greater loss of RNFL thickness between baseline and 3 months predicted lower final RNFL thickness (for every $1\mu\text{m}$ of loss between baseline and 3 months there was $1.05\mu\text{m}$ of loss at 12 months, 95% CI 0.78 , 1.32 ; $P<0.001$). This effect was similar in those with good and poor recovery.

Relationship of early swelling to later RNFL loss

The degree of swelling (i.e. affected minus fellow eye values) observed in the RNFL at baseline did not determine degree of RNFL reduction compared with the fellow eye at 12 months (observed coefficient $0.13\mu\text{m}$ of RNFL loss observed at 12 months for every $1\mu\text{m}$ of RNFL swelling at baseline, 95% CI -0.02 , 0.28 ; $P=0.093$), nor did the degree of swelling in the macula influence the eventual macular volume (observed coefficient 0.14 mm^3 of macular volume loss at 12 months for every 1 mm^3 of macular volume swelling at baseline, 95% CI -0.42 , 0.14 ; $P=0.754$).

Relationships with vision

Higher baseline RNFL thickness of the affected eye was associated with (i) worse baseline logMAR visual acuity (logMAR acuity 0.007 units higher for $1\mu\text{m}$ increase in RNFL thickness, 95% CI 0.001 , 0.014 ; $P=0.020$); (ii) lower baseline visual mean field deviation (visual field mean deviation 0.129 dB lower for each $1\mu\text{m}$

Table 3 Estimated rates of reduction in macular volume

Time (from first measurement)	Rate of atrophy (mm ³ per month)	95% CI	P-value
At first measurement	−0.33	−0.50–0.02	<0.05
15 days	−0.27	−0.45–0.16	<0.01
1 month	−0.22	−0.33–0.14	<0.01
3 months	−0.09	−0.13–0.06	<0.001
4 months	−0.06	−0.09–0.04	<0.001
5 months	−0.04	−0.07–0.02	<0.001
6 months	−0.03	−0.05–0.01	<0.001
12 months	−0.002	−0.007–0.000	<0.01

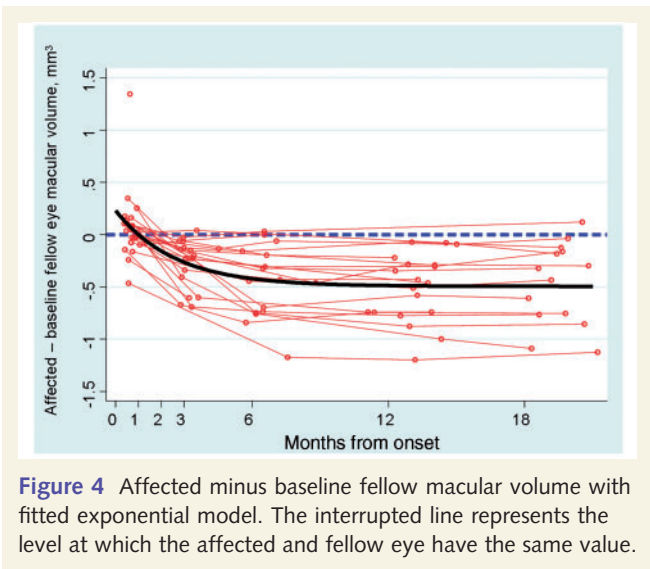


Figure 4 Affected minus baseline fellow macular volume with fitted exponential model. The interrupted line represents the level at which the affected and fellow eye have the same value.

increase in RNFL thickness, 95% CI −0.227, −0.031; $P = 0.009$; Fig. 5); and (iii) worse colour vision (for each 1 μm increase in RNFL thickness, $\sqrt{\text{TES}}$ increased by 0.118, 95% CI 0.029, 0.205; $P = 0.012$). Baseline macular volume was not correlated with logMAR visual acuity ($P = 0.526$) or colour vision ($P = 0.781$). The relationship of macular volume and whole visual field was not tested as it was felt that this was biologically inappropriate. No single quadrant of the RNFL was a better predictor of visual acuity or colour vision at baseline than the circumpapillary (whole) RNFL measure.

At 12 months, lower RNFL thickness was associated with: (i) worse logMAR acuity (observed coefficient −0.008, 95% CI −0.017, 0.000; $P = 0.018$); (ii) lower visual field mean deviation (observed coefficient 0.194, 95% CI −0.016, 0.403; $P = 0.023$); and (iii) worse colour vision (for each 1 μm decrease in RNFL thickness, $\sqrt{\text{TES}}$ decreased by 0.236, 95% CI 0.134, 0.334; $P < 0.001$). At the same time, lower macular volume was associated with worse colour vision (for each 1 mm^3 reduction in macular volume, $\sqrt{\text{TES}}$ decreased by 8.71, 95% CI 4.11, 13.3; $P = 0.004$), but not logMAR acuity ($P = 0.114$). The degree of RNFL swelling at baseline did not predict either logMAR acuity (observed coefficient 0.00 95% CI 0.00, 0.00; $P = 0.899$) or

visual field mean deviation (observed coefficient −0.13, 95% CI −0.08, 0.05; $P = 0.667$) at 12 months.

Higher (i.e. worse) baseline logMAR acuity was associated with lower RNFL thickness at 12 months (RNFL thickness 1.42 μm lower for every 0.1 increase in logMAR acuity, 95% CI 0.58, 2.26; $P = 0.002$; $R^2 = 0.43$), and higher baseline Sloan 1.25% contrast acuity was associated with lower RNFL thickness at 12 months (RNFL thickness 2.24 μm lower for every 0.1 increase in Sloan 1.25% contrast acuity, 95% CI 0.21, 4.28; $P = 0.033$, $R^2 = 0.30$).

Association with visual evoked potentials

At baseline, higher diseased RNFL thickness predicted longer visual evoked potential latency (visual evoked potential latency 0.266 ms longer for each 1 μm increase in RNFL thickness, 95% CI 0.072, 0.460; $P = 0.040$). The relationship between diseased RNFL thickness and visual evoked potential amplitude did not reach significance (observed coefficient 0.043 mV decrease in visual evoked potential amplitude for every 1 μm increase in RNFL thickness, 95% CI −0.082, −0.003; $P = 0.076$). At 6 months, lower diseased RNFL thickness was associated with lower visual evoked potential amplitude (observed coefficient 0.109 mV decrease in visual evoked potential amplitude for every 1 μm decrease in RNFL thickness, 95% CI 0.003, 0.217; $P = 0.045$), but there was no significant relationship between visual evoked potential latency and RNFL thickness (observed coefficient visual evoked potential latency 0.077 ms longer for every 1 μm decrease in RNFL thickness, 95% CI −0.053, 0.378; $P = 0.721$). At 12 months, lower diseased RNFL thickness was associated with lower visual evoked potential amplitude (observed coefficient 0.166 mV decrease in visual evoked potential amplitude for every 1 μm decrease in RNFL thickness, 95% CI 0.053, 0.279; $P = 0.009$), but there was no relationship between visual evoked potential latency and diseased RNFL thickness (observed coefficient −0.123, 95% CI −0.623, 0.376; $P = 0.609$).

Sample size estimates

Sample size calculations used the following estimates from the data, for 3, 6 and 12 months, respectively: affected eye RNFL SD 16.16, 18.32 and 16.34 μm ; mean (SD) of the affected–baseline unaffected RNFL −10.00 (12.45), −19.20 (14.42), −18.95 (14.51) μm ; Pearson correlation coefficients 0.65, 0.63, 0.48.

Sample size estimates for the three different trial designs at 3, 6 and 12 months are given in Table 4. The design which adjusted for the fellow eye value and used analysis of covariance (Method C) analysis was the most powerful, followed by the comparison of affected eye–fellow eye differences. The study design with no adjustment for fellow eye values (Method A) was the least powerful. For Method C, with 12-month duration, 80% power and 30 and 50% treatment effects, sample sizes were 100 (95% CI 56, 246) and 36 (95% CI 20, 89), respectively; and for 6-month duration, corresponding sample sizes were 97 (95% CI 54, 197) and 35 (95% CI 20, 71).

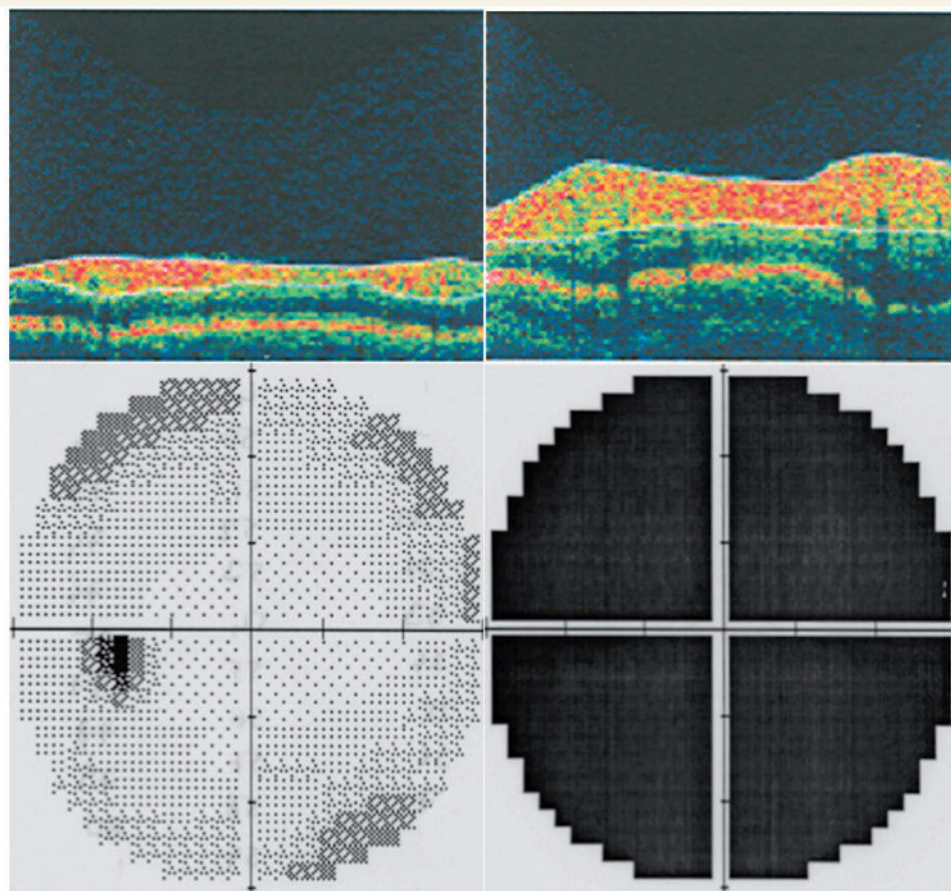


Figure 5 Optical coherence tomography images of the RNFL of a patient taken 12 days after the onset of symptoms of right-sided acute optic neuritis, with accompanying visual field demonstrating the poor vision associated with severe swelling of the RNFL. The RNFL thickness and visual fields of the unaffected left eye are normal.

Discussion

In this study, we have documented the time course of changes in the retina following optic neuritis and demonstrated the rapid change from swelling to atrophy in the RNFL, which occurs in the first months after optic neuritis. From the data presented here, it appears that thinning of the affected eye RNFL relative to the fellow eye first typically appears within 1–2 months (Fig. 2) and at least half of the eventual RNFL loss that occurs is evident after 3 months (Table 1). This finding is in keeping with earlier studies serially examining optic nerve mean area following optic neuritis (Hickman *et al.*, 2004a), and with pathological studies indicating the proportion of axonal loss is greatest in early and acutely inflammatory lesions (Ferguson *et al.*, 1997; Kornek *et al.*, 2000). The model predicts that there is an ongoing but very slow rate of loss at 12 months, which is concordant with radiological (Hickman *et al.*, 2004a) and pathological data suggesting a low grade inflammation and axonal loss which persists for some time following the acute inflammatory episode (Kornek *et al.*, 2000). This may also be due, in part, to a post-inflammatory phase in which the axon is demyelinated and lacking the trophic support of oligodendrocytes (Wilkins and Compston, 2005) and vulnerable to toxicity from compounds such as nitric

oxide (Smith *et al.*, 2001). There may also be ongoing atrophy with slow clearance of phagocytosed debris associated with Wallerian degeneration.

The speed of RNFL thinning in the first 3 months was significantly greater in those patients with an eventual poor recovery. The decrease in RNFL thickness seen in the whole period of this study, occurring from a baseline of swelling in the RNFL, is probably composed of two components: resolution of inflammation and oedema on the one hand and loss of tissue due to axonal death and Wallerian degeneration on the other. Although it is not possible to establish which component predominates in the early months (optical coherence tomography does not distinguish between these two processes), because the extent of swelling *per se* did not predict visual recovery, it seems that the more rapid decline in RNFL thickness in the poor recovery group reflects a greater extent of early axonal loss in this cohort (which was also confirmed to have greater axonal loss at a much later time point, when inflammation should no longer be present). By 3 months, the patients with an eventual poor visual recovery had a lower RNFL thickness than the remainder of the patients ($75.5\mu\text{m}$ for poor recovery versus $99.7\mu\text{m}$ for good recovery, $P < 0.002$).

Interpretation of the model of retinal changes must be accompanied by a number of caveats. First, there are only two measures

Table 4 Sample size estimates for outcome measures (retinal nerve fibre layer thickness) at 12 months (panel a), 6 months (panel b) and 3 months (panel c) for a parallel-groups, placebo-controlled trial

Effect size	80% power			90% power		
	Method			Method		
	A	B	C	A	B	C
Panel a						
20	292	231	225	391	309	301
30	130	103	100	174	137	134
40	73	58	57	98	78	76
50	47	37	36	63	50	49
60	33	26	25	44	35	34
70	24	19	19	32	26	25
80	19	15	15	25	20	19
Panel b						
20	358	222	218	479	297	292
30	159	99	97	213	132	130
40	90	56	55	120	75	73
50	58	36	35	77	48	47
60	40	25	25	54	33	33
70	30	19	18	40	25	24
80	23	14	14	30	19	19
Panel c						
20	1024	608	596	1370	814	797
30	455	271	265	609	362	355
40	256	152	149	343	204	200
50	164	98	96	220	131	128
60	114	68	67	153	91	89
70	84	50	49	112	67	66
80	64	38	38	86	51	50

Effect size: percent decrease in retinal nerve fibre layer loss comparing neuroprotective treatment versus placebo arm. Method A: Comparison of follow-up affected eye retinal nerve fibre layer, ignoring fellow eye value, as would be advisable when there is a history of prior optic neuritis in the fellow eye; this calculation requires the standard deviation of follow-up affected eye retinal nerve fibre layer. Method B: Comparison of difference between follow-up affected eye and baseline fellow eye retinal nerve fibre layer; this calculation requires the standard deviation of this difference. Method C: Comparison of follow-up affected eye adjusted for baseline fellow eye retinal nerve fibre layer; this calculation requires the follow-up affected eye retinal nerve fibre layer standard deviation and the Pearson correlation coefficient for follow-up affected versus baseline fellow eye retinal nerve fibre layer (analysis of covariance).

in the earliest phases following the onset of symptoms, which may diminish the accuracy of the model during this period. Further study with frequent imaging during the first 3 months should provide a more reliable model of early RNFL changes and their relationship to concurrent and future visual function. Secondly, newer optical coherence tomography systems that provide greater resolution of the retinal layers may also be informative (Drexler and Fujimoto, 2008), and the model may not apply to other optical coherence tomography devices, which return different values for the retina (Wolf-Schnurbusch *et al.*, 2009). The confidence intervals are wide for some of the estimated parameters in this study.

Thirdly, the exponential model reported is limited in not estimating between-subject variation in the γ parameter and between-subject covariance between the α and β parameters; a larger sample size would be required to estimate these and thus

obtain meaningful, accurate information on between-subject variation in the parameters and the quantities dependent on them. However, we believe the parameter estimates themselves are robust to this limitation and are supported by the alternative models we fitted.

Fourthly, the sample size of our cohort resulted in only a small number of subjects with poor recovery, which may explain why the model did not distinguish the trajectory of the changes in their RNFL from those with a good outcome, except by the eventual value. However, the proportion of subjects with a poor outcome (5/23; 21%) is very typical of what is seen in acute demyelinating optic neuritis. Furthermore, the whole cohort exhibited age, gender and brain MRI findings that all accord with that described in a typical young adult cohort presenting with an acute unilateral episode of optic neuritis. Overall, the cohort studied would seem to provide a robust description of the longitudinal changes that occur in the RNFL following acute demyelinating optic neuritis.

We have also applied a modelling approach in previous longitudinal studies of optic neuritis to investigate the evolution of optic nerve MRI measures (Hickman *et al.*, 2004a); it would be of interest to apply modelling in future studies to investigate the evolution of measures of visual function or visual evoked potentials.

The macular volume changes seen here suggest that following optic neuritis, there is not only loss of axons but also of retinal ganglion cell bodies. The ganglion cell layer forms a substantial portion of the retina at the macula, and the loss of macula volume seen in this cohort following optic neuritis suggests that retinal ganglion cell loss is also occurring. There may be loss of other components of the retina at the macula causing loss of volume, but this seems less likely. Quantification of the changes in the ganglion cell layer following optic neuritis may be possible with newer generation optical coherence tomography devices (Tan *et al.*, 2009).

Whereas increased swelling at baseline was associated with both reduced vision and prolonged visual evoked potential latency during the acute phase, it did not predict later axonal loss as measured by reduced RNFL thickness. The best predictor of eventual RNFL thickness was the loss of RNFL thickness in the interval between the baseline and 3-month time point, of itself not particularly unexpected, as the majority of the decrease had occurred by this point. The association of increased RNFL thickness with a contemporaneously increased visual evoked potential latency and visual loss suggests that there the severity of inflammation and/or impaired axonal transport (RNFL swelling) relates to the severity of demyelination (long latency visual evoked potential) and conduction block (visual loss) during the acute phase of optic neuritis.

Using the serial RNFL measurements observed in this study, we generated sample sizes for putative clinical trials of acute neuroprotective agents in optic neuritis. Whilst significant RNFL thinning had occurred by 3 months, a further substantial decrease in RNFL thickness is evident after 6 months (Table 1) and the required sample sizes are appreciably lower if outcome is measured at 6 months (Table 4). However, there appears to be no useful advantage in terms of sample size reduction in extending a trial to longer than 6 months, which reflects the minimal RNFL loss observed after this period. Our calculations suggest the numbers

required in such a trial are substantially smaller if outcome measures can be adjusted for a clinically unaffected fellow eye. This outcome measure overcomes the large inter-subject variability in normal RNFL thickness that will impact sample size calculations using the absolute RNFL measure as an outcome. Overall sample sizes for detecting a moderate 50% neuroprotective effect at 6 months—inferred from a 50% reduction in the amount of RNFL loss compared to the fellow eye in a trial comparing active and placebo arms—are ~35 per arm (95% CI ~20, 70) with 80% power and ~50 per arm (CI ~30, 110) with 90% power. The equivalent sample sizes for a lesser 30% neuroprotective effect at 6 months are ~100 (CI ~55, 200) and ~130 (CI ~70, 300) per arm.

When the fellow eye has already experienced an episode of optic neuritis, the final inter-eye difference is likely to be small and the actual RNFL measure of the affected eye will likely be the more suitable outcome measure, with a consequent higher sample size for the study design. Our cohort presented with clinically isolated unilateral optic neuritis and the unaffected fellow eye did not show RNFL thinning compared with controls; however, in established relapsing remitting multiple sclerosis cohorts, where RNFL reductions have been reported in fellow eyes (Fisher *et al.*, 2006; Pulicken *et al.*, 2007), the inter-eye RNFL thickness difference may be a less powerful outcome measure. Our cohort did not receive intravenous glucocorticosteroid treatment for their optic neuritis, although the lack of benefit of such an intervention on either final visual function (Beck and Cleary, 1993) and on optic nerve cross-sectional area (Hickman *et al.*, 2003) suggest that its effect, if any, on the RNFL would be small. Overall, optical coherence tomography-measured RNFL loss would appear to be a feasible and objective outcome measure for evaluating putative experimental neuroprotective treatments in acute optic neuritis.

Acknowledgements

The authors thank the study participants.

Funding

The NMR Research Unit is supported by the Multiple Sclerosis Society of Great Britain and Northern Ireland and the Department of Health's Comprehensive Biomedical Research Centre at University College Hospitals Trust. P. G. Schlottmann was supported by The Guide Dogs for the Blind Association.

Supplementary material

Supplementary material is available at *Brain* online.

References

- Baleanu D, Tornow RP, Horn FK, Laemmer R, Roessler CW, Juennemann AG, *et al.* Retinal nerve fiber layer thickness in normals measured by spectral domain OCT. *J Glaucoma* 2009; Epub ahead of print: doi:10.1097/IJG.0b013e3181c4b0c7; PMID: 20051888.
- Beck RW, Cleary PA. Optic neuritis treatment trial. One-year follow-up results. *Arch Ophthalmol* 1993; 111: 773–5.
- Beck RW, Cleary PA, Backlund JC. The course of visual recovery after optic neuritis. Experience of the Optic Neuritis Treatment Trial. *Ophthalmology* 1994; 101: 1771–8.
- Brusa A, Jones SJ, Plant GT. Long-term remyelination after optic neuritis: a 2-year visual evoked potential and psychophysical serial study. *Brain* 2001; 124: 468–79.
- Casella G, George E. Explaining the Gibbs sampler. *Am Stat* 1992; 46: 167–74.
- Costello F, Coupland S, Hodge W, Lorello GR, Koroluk J, Pan YI, *et al.* Quantifying axonal loss after optic neuritis with optical coherence tomography. *Ann Neurol* 2006; 59: 963–9.
- Costello F, Hodge W, Pan YI, Eggenberger E, Coupland S, Kardon RH. Tracking retinal nerve fiber layer loss after optic neuritis: a prospective study using optical coherence tomography. *Mult Scler* 2008; 14: 893–905.
- Drexler W, Fujimoto JG. State-of-the-art retinal optical coherence tomography. *Prog Retin Eye Res* 2008; 27: 45–88.
- Efron B, Tibshirani RJ. An introduction to the bootstrap. New York: Chapman & Hall; 1993.
- Farnsworth D. The Farnsworth-Munsell 100-hue and dichotomous tests for colour vision. *J Opt Soc Am* 1943; 33: 568–74.
- Ferguson B, Matyszak MK, Esiri MM, Perry VH. Axonal damage in acute multiple sclerosis lesions. *Brain* 1997; 120(Pt 3): 393–9.
- Ferris FL 3rd, Kassoff A, Bresnick GH, Bailey I. New visual acuity charts for clinical research. *Am J Ophthalmol* 1982; 94: 91–6.
- Fisher JB, Jacobs DA, Markowitz CE, Galetta SL, Volpe NJ, Nano-Schiavi ML, *et al.* Relation of visual function to retinal nerve fiber layer thickness in multiple sclerosis. *Ophthalmology* 2006; 113: 324–32.
- Frisén L, Hoyt WF. Insidious atrophy of retinal nerve fibers in multiple sclerosis. Funduscopy identification in patients with and without visual complaints. *Arch Ophthalmol* 1974; 92: 91–7.
- Hickman SJ, Kapoor R, Jones SJ, Altmann DR, Plant GT, Miller DH. Corticosteroids do not prevent optic nerve atrophy following optic neuritis. *J Neurol Neurosurg Psychiatry* 2003; 74: 1139–41.
- Hickman SJ, Toosy AT, Jones SJ, Altmann DR, Miszkil KA, MacManus DG, *et al.* A serial MRI study following optic nerve mean area in acute optic neuritis. *Brain* 2004a; 127: 2498–505.
- Hickman SJ, Toosy AT, Miszkil KA, Jones SJ, Altmann DR, MacManus DG, *et al.* Visual recovery following acute optic neuritis—a clinical, electrophysiological and magnetic resonance imaging study. *J Neurol* 2004b; 251: 996–1005.
- Hood DC, Fortune B, Arthur SN, Xing D, Salant JA, Ritch R, *et al.* Blood vessel contributions to retinal nerve fiber layer thickness profiles measured with optical coherence tomography. *J Glaucoma* 2008; 17: 519–28.
- Huang D, Swanson EA, Lin CP, Schuman JS, Stinson WG, Chang W, *et al.* Optical coherence tomography. *Science* 1991; 254: 1178–81.
- Huber P.J. The behavior of maximum likelihood estimates under non-standard conditions. In: *Proceedings of the Fifth Berkeley Symposium on Mathematical Statistics and Probability*. Vol. 3. Berkeley, CA: University of California Press; 1967. p. 221–33.
- Kallenbach K, Simonsen H, Sander B, Wanscher B, Larsson H, Larsen M, *et al.* Retinal nerve fiber layer thickness is associated with lesion length in acute optic neuritis. *Neurology* 2010; 74: 252–8.
- Kaushik S, Pandav SS, Ichhpujani P, Gupta A. Fixed-diameter scan protocol preferable for retinal nerve fibre layer measurement by optical coherence tomography in all sizes of optic discs. *Br J Ophthalmol* 2009; 93: 895–900.
- Klistorner A, Arvind H, Nguyen T, Garrick R, Paine M, Graham S, *et al.* Axonal loss and myelin in early ON loss in postacute optic neuritis. *Ann Neurol* 2008; 64: 325–31.
- Kolappan M, Henderson A, Jenkins T, Wheeler-Kingshott C, Plant G, Thompson A, *et al.* Assessing structure and function of the afferent

- visual pathway in multiple sclerosis and associated optic neuritis. *J Neurol* 2009; 256: 305–19.
- Kornek B, Storch MK, Weissert R, Wallstroem E, Stefferl A, Olsson T, et al. Multiple sclerosis and chronic autoimmune encephalomyelitis: a comparative quantitative study of axonal injury in active, inactive, and remyelinated lesions. *Am J Pathol* 2000; 157: 267–76.
- Kupersmith MJ, Alban T, Zeiffer B, Lefton D. Contrast-enhanced MRI in acute optic neuritis: relationship to visual performance. *Brain* 2002; 125: 812–22.
- Lunn DJ, Thomas A, Best N, Spiegelhalter D. WinBUGS – a Bayesian modelling framework: concepts, structure, and extensibility. *Stat Comput* 2000; 10: 325–37.
- Menke MN, Feke GT, Trempe CL. OCT measurements in patients with optic disc edema. *Invest Ophthalmol Vis Sci* 2005; 46: 3807–11.
- Ogden TE. Nerve fiber layer of the primate retina: morphometric analysis. *Invest Ophthalmol Vis Sci* 1984; 25: 19–29.
- Optic Neuritis Study Group. The clinical profile of optic neuritis. Experience of the Optic Neuritis Treatment Trial. *Arch Ophthalmol* 1991; 109: 1673–8.
- Parisi V, Manni G, Spadaro M, Colacino G, Restuccia R, Marchi S, et al. Correlation between morphological and functional retinal impairment in multiple sclerosis patients. *Invest Ophthalmol Vis Sci* 1999; 40: 2520–7.
- Polman CH, Reingold SC, Edan G, Filippi M, Hartung HP, Kappos L, et al. Diagnostic criteria for multiple sclerosis: 2005 revisions to the “McDonald Criteria”. *Ann Neurol* 2005; 58: 840–6.
- Pro MJ, Pons ME, Liebmann JM, Ritch R, Zafar S, Lefton D, et al. Imaging of the optic disc and retinal nerve fiber layer in acute optic neuritis. *J Neurol Sci* 2006; 250: 114–9.
- Pulicken M, Gordon-Lipkin E, Balcer LJ, Frohman E, Cutter G, Calabresi PA. Optical coherence tomography and disease subtype in multiple sclerosis. *Neurology* 2007; 69: 2085–92.
- Senn SJ. Statistical methods in drug development. Chichester: Wiley; 1997.
- Sharpe JA, Sanders MD. Atrophy of myelinated nerve fibres in the retina in optic neuritis. *Br J Ophthalmol* 1975; 59: 229–32.
- Smith KJ, Kapoor R, Hall SM, Davies M. Electrically active axons degenerate when exposed to nitric oxide. *Ann Neurol* 2001; 49: 470–6.
- Snedecor G, Cochran W. Statistical methods. 8th edn, Ames, IA: Iowa State University Press; 1989.
- Tan O, Chopra V, Lu AT, Schuman JS, Ishikawa H, Varma R, et al. Detection of macular ganglion cell loss in glaucoma by Fourier-domain optical coherence tomography. *Ophthalmology* 2009; 116: 2305–10.
- Trapp BD, Peterson J, Ransohoff RM, Rudick R, Mork S, Bo L. Axonal transection in the lesions of multiple sclerosis. *N Engl J Med* 1998; 338: 278–85.
- Trip SA, Schlottmann PG, Jones SJ, Altmann DR, Garway-Heath DF, Thompson AJ, et al. Retinal nerve fiber layer axonal loss and visual dysfunction in optic neuritis. *Ann Neurol* 2005; 58: 383–91.
- Trobe JD, Beck RW, Moke PS, Cleary PA. Contrast sensitivity and other vision tests in the optic neuritis treatment trial. *Am J Ophthalmol* 1996; 121: 547–53.
- White H. A heteroskedasticity-consistent covariance matrix estimator and a direct test for heteroskedasticity. *Econometrica* 1980; 48: 817–30.
- Wilkins A, Compston A. Trophic factors attenuate nitric oxide mediated neuronal and axonal injury in vitro: roles and interactions of mitogen-activated protein kinase signalling pathways. *J Neurochem* 2005; 92: 1487–96.
- Wolf-Schnurrbusch UEK, Ceklic L, Brinkmann CK, Iliev ME, Frey M, Rothenbuehler SP, et al. Macular thickness measurements in healthy eyes using six different optical coherence tomography instruments. *Invest Ophthalmol Vis Sci* 2009; 50: 3432–7.